nature chemistry

ARTICLES

PUBLISHED ONLINE: 10 MAY 2009 | DOI: 10.1038/NCHEM.207

Force-activated reactivity switch in a bimolecular chemical reaction

Sergi Garcia-Manyes[1]*, Jian Liang[1], Robert Szoszkiewicz[1], Tzu-Ling Kuo[2] and Julio M. Fernández[1]*

The effect of mechanical force on the free-energy surface that governs a chemical reaction is largely unknown. The combination of protein engineering with single-molecule force-clamp spectroscopy allows us to study the influence of mechanical force on the rate at which a protein disulfide bond is reduced by nucleophiles in a bimolecular substitution reaction (S_N2). We found that cleavage of a protein disulfide bond by hydroxide anions exhibits an abrupt reactivity 'switch' at ~500 pN, after which the accelerating effect of force on the rate of an S_N2 chemical reaction greatly diminishes. We propose that an abrupt force-induced conformational change of the protein disulfide bond shifts its ground state, drastically changing its reactivity in S_N2 chemical reactions. Our experiments directly demonstrate the action of a force-activated switch in the chemical reactivity of a single molecule.

The energy required for a chemical reaction to proceed is commonly provided by heat, light, electric potential or pressure[1,2]. This energy allows the colliding molecules to overcome the activation-energy barrier that governs the chemical reaction. Mechanical force is a distinct, albeit less explored, way to activate a chemical reaction because it can deform the reacting molecules along a well-defined direction of the reaction coordinate[1]. Indeed, activation of covalent bonds on the application of force to the reacting system by means of ultrasound was recently shown to change the reaction pathways substantially, and leads to reaction products that are different from those obtained when the reaction is initiated by heat or light[2]. However, in these experiments the magnitude and direction of the applied forces were not known. Furthermore, calculations of the density functions in the gas phase show how the application of relatively low forces can induce a substantial change in the energy profile of a chemical reaction[3].

At the single-molecule level, experiments conducted with atomic force microscopy (AFM)[4–6], supported by quantum-level simulations, measured the mechanical forces required for homolytic and heterolytic bond rupture[7]. These studies show a continuous deformation of covalent bonds along a one-dimensional Morse-like potential with the application of a force[6,8]. In addition to these observations, the vast single-molecule literature that has accumulated over the past ten years demonstrates the ability of mechanical forces to drive conformational changes in a diverse set of molecules, including DNA, RNA, polysaccharides and proteins[9–16]. In spite of these advances, the relationship between force-driven molecular conformations and complex chemical reactions remains poorly understood.

A combination of protein-engineering techniques with single-molecule force-clamp spectroscopy has made it possible to monitor the reduction of individual disulfide bonds embedded within a protein structure[17,18]. Our work at the single-bond level directly demonstrated that the reduction of a protein disulfide bond by a nucleophile is a force-dependent S_N2 chemical reaction[17]. These early experiments were carried out over a range of pulling forces up to 500 pN, and showed that the rate of disulfide-bond reduction increased exponentially with the pulling force, in excellent agreement with a simple Arrhenius description of the energy barrier that governs the reaction[19]. The main advantage of this experimental approach is that it probes the transition state of the reaction with a calibrated mechanical force and sub-ångström resolution[19]. For example, we measured distances to the transition state (Δx_r) of the S_N2 reaction that were in good agreement with quantum chemical calculations of the elongation experienced by the disulfide bond at the transition state of the reaction[19]. In our early experiments, the rate of disulfide-bond reduction by nucleophiles always followed a simple exponential increase with the applied force, which marks a single well-defined transition state for the reaction.

Here, we demonstrate that with hydroxide anions as the nucleophiles we can greatly extend the range of forces over which the S_N2 reduction of disulfide bonds can be studied (to 2,000 pN). Surprisingly, we found that the reduction of protein disulfide bonds exhibits two distinct transition states that switch from one to the other at a force of 500 pN. Our data show that at low pulling forces (<500 pN) the reaction rate is limited by an energy barrier with $\Delta x_r \sim 0.5$ Å, but at higher forces (>500 pN) a different energy barrier dominates, with a much shorter Δx_r, ~0.1 Å. Our results uncover a force-activated molecular switch that greatly affects the reactivity of an S_N2 chemical reaction. Our experiments also illustrate the remarkable ability of force-clamp spectroscopy to capture previously inaccessible details of the energy profile of a protein-based chemical reaction.

Results

Using the experimental protocol of our previous studies, we engineered two point mutations (Gly32Cys and Ala75Cys) into the 27th immunoglobulin-like domain of cardiac titin (I27), the mechanical properties of which have been extensively characterized[20]. We constructed and expressed a polyprotein that consisted of eight identical repeats of this modified domain, $(I27_{G32C-A75C})_8$. In this construct, each folded domain contains a single disulfide bond that is buried and inaccessible to the external solvent environment. In our force-clamp assay, we used a two-pulse force protocol to study the force-dependent kinetics of the disulfide reduction[17,21] (Fig. 1a). The first force pulse (180 pN) rapidly unfolded all of the modules in the polyprotein. Each unfolding event was marked by a step increase in length of ~11 nm, which corresponds to the extension

[1]Department of Biological Sciences, [2]Department of Physics, Columbia University, New York, New York 10027, USA.
*e-mail: sergi@biology.columbia.edu; jfernandez@columbia.edu

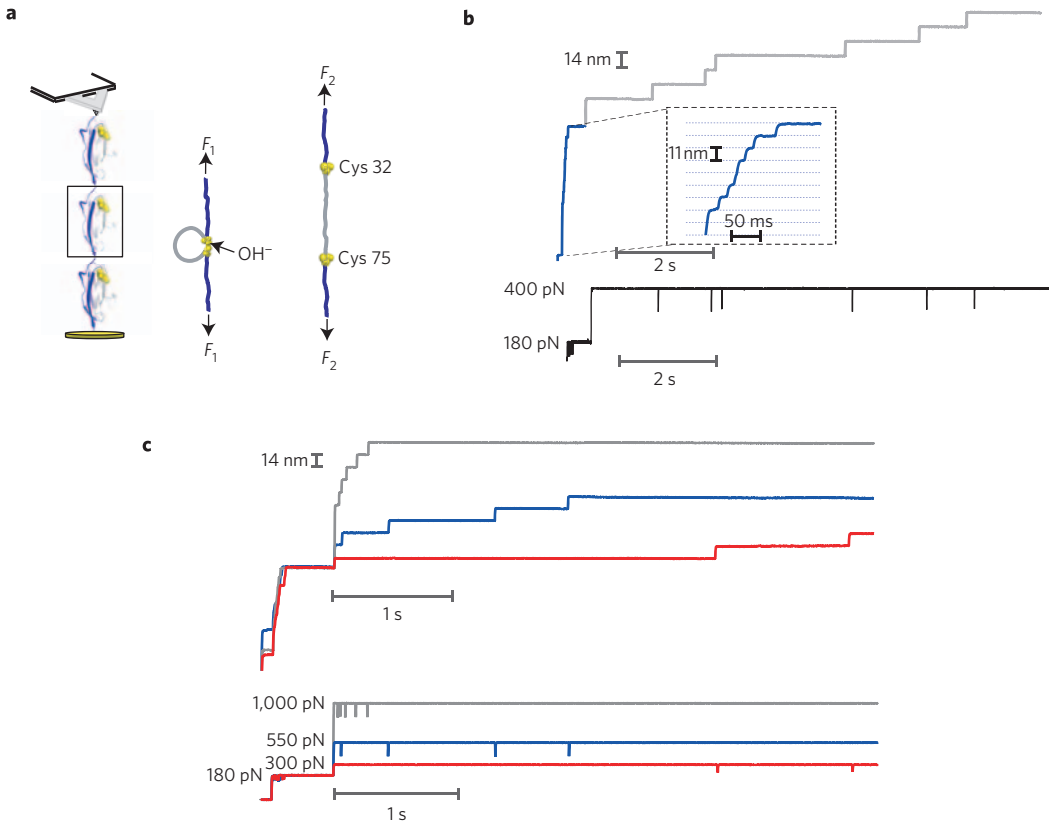

Figure 1 | Force-clamp spectroscopy monitors events in the reduction of single disulfide bonds with hydroxide anions in the solution. a, An AFM cantilever picks up a polyprotein that contains eight repeats of the I27 module with disulfide bonds formed between cysteine residues engineered into positions 32 and 75. **b**, Using a double-pulse protocol (F_1 and F_2), we measured the rate at which the polyprotein disulfide bond was reduced by hydroxide anions. The first force pulse ($F_1 = 180$ pN) unfolds and extends all the modules of the $(I27_{G32C\text{-}A75C})_8$ polyprotein to the mechanical clamp created by the disulfide bonds, which exposes them to the solution (blue line). Each unfolding event is marked by a step increase of ~11 nm (inset, blue line, horizontal scale 50 ms). A second, stronger force pulse tracks the time course of the disulfide-bond reduction, fingerprinted by equally spaced 14-nm steps that correspond to the extension of the peptide chain released on the reduction of each disulfide bond (grey line). **c**, The rate of disulfide-bond reduction is accelerated by the stretching force, as is apparent from the time course of disulfide reduction observed at 300 pN (red trajectory), $F_2 = 550$ pN (blue trajectory) and $F_2 = 1{,}000$ pN (grey trajectory).

of the amino acids of the $I27_{G32C–A75C}$ protein up to the disulfide bond. Unfolding exposes the buried disulfide bond to the solution, which allows nucleophilic attack and thus reduction of the exposed disulfide bonds (Fig. 1b, blue lines). Shortly after we had ensured the unfolding of all the modules in the polyprotein, we applied second force pulses of up to 2,000 pN to examine the force dependency of the rate of reduction. In the presence of hydroxide anions (~0.25 mM, pH 11.4), the reduction of each disulfide bond is marked by a ~14 nm elongation step (Fig. 1b, grey line) that corresponds exactly to the total length of the residues trapped behind the disulfide bond.

We varied the applied constant force of the second pulse and measured the kinetics of disulfide reduction promoted by the hydroxide anions. As is clear from Fig. 1c, the rate of reduction is strongly influenced by force, rapidly increasing as the force is increased from 300 pN (red trace) to 1,000 pN (grey trace). We have not observed the ~14 nm steps at neutral pH, at which the concentration of hydroxide anions is vanishingly small ($\sim 10^{-7}$ M). To obtain the rate of reduction at any particular force or hydroxide anion concentration, we averaged and normalized 30–50 individual traces, such as those shown in Fig. 1, and fitted the average trajectory to a single exponential (dotted lines in Fig. 2a,b). From the exponential time constant of the fits (τ_R) we calculated the rate of reduction as $r = 1/\tau_R$. The standard error of the mean (s.e.m.) of these data was estimated by bootstrapping. As before, we fitted the force dependency of the rate of reduction using the simple Arrhenius term $r(F) = r(0)\exp(F\Delta x_r/kT)$, where $r(0)$ is the rate constant in the absence of force[17,19].

A semilogarithmic plot of the rate versus force measurements at pH 11.4 and over an expanded force range up to 2,000 pN (Fig. 2c) shows two clearly distinct regions marked by significantly different exponential dependencies on the pulling force. It is clear that a single Arrhenius term cannot fit the data of Fig. 2c. The first regime of this plot, comprising data up to a force of 500 pN, is described well by an Arrhenius term with $\Delta x_r = 0.50$ Å and $r(0) = 8.2 \times 10^{-4}\ s^{-1}$. However, fitting the Arrhenius term to the data at forces higher than 500 pN revealed a novel conformation of the transition state with a much shorter distance, $\Delta x_r = 0.11$ Å, and $r(0) = 0.13\ s^{-1}$.

These experiments were repeated at different pH values to allow us to measure the force-dependent reduction rate over a range of hydroxide anion concentrations (Fig. 3a,b). As the pH is increased (for example, pH > 13, Fig. 3a), the measured rate of reduction at high forces approaches the upper rate limit of our spectrometer ($10–20\ s^{-1}$). Similarly, at lower pH values (~11), the rate of reduction measured at low forces is near the lower rate limit of the instrument ($\sim 0.05\ s^{-1}$). Nonetheless, the abrupt switch between force regimes of the reaction is clear in all cases, at ~500 pN (grey bar, Fig. 3a). The rate–force curves obtained at different values of pH (Fig. 3a) are simply shifted with respect to each other by the different

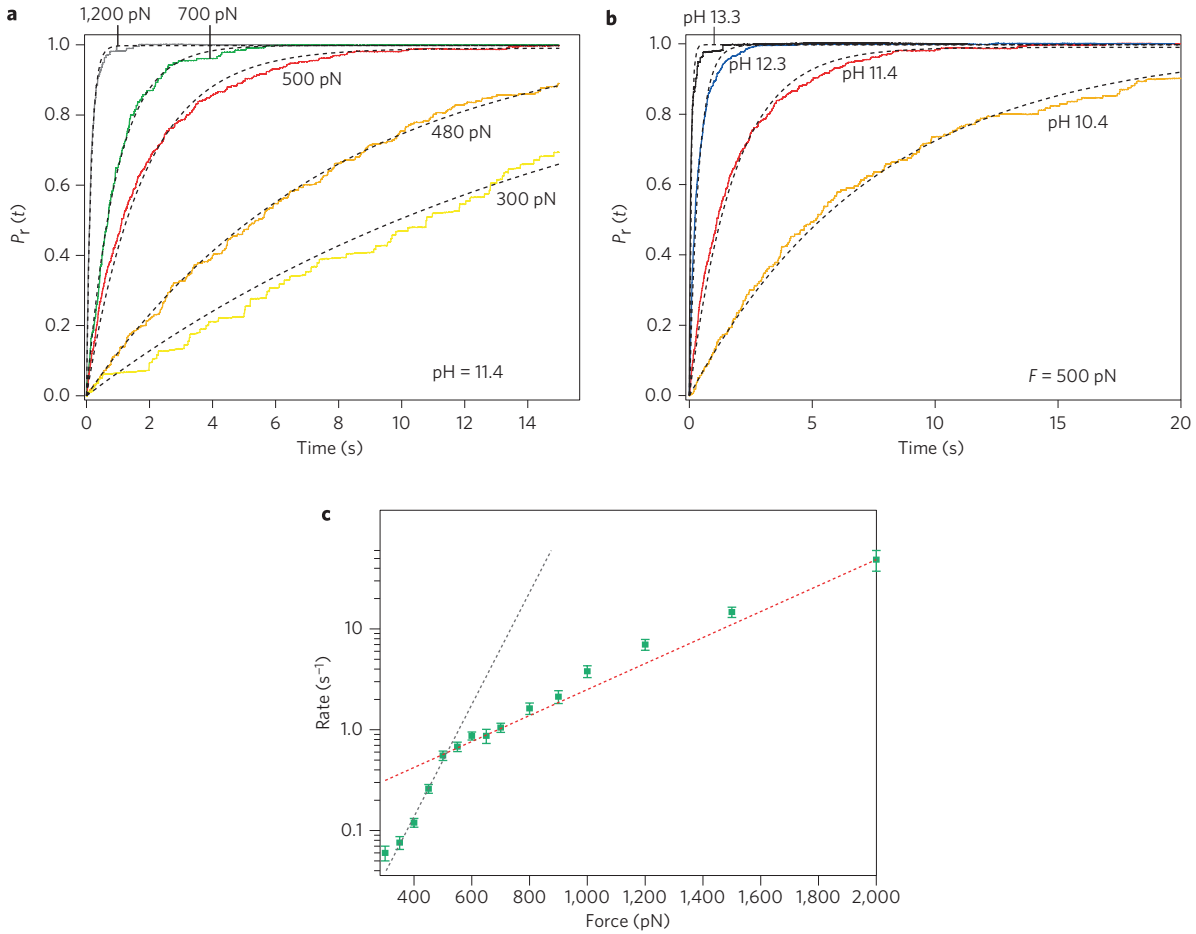

Figure 2 | The force dependency of the rate of disulfide-bond reduction by hydroxide anions exhibits two distinct reactivity regimes that switch at 500 pN. a, Measurement of the rate of disulfide-bond reduction at a constant pH of 11.4, at different pulling forces (range 300–1,200 pN). At each force we averaged and normalized an ensemble of 30–50 traces obtained during the second force pulse (Fig. 1c) to obtain the probability of reduction, P_r. The reduction rate at each pulling force is obtained by fitting a single exponential to the averaged trace (dotted black lines). **b**, Similar measurement of the rate of reduction at a constant force of 500 pN, at different values of pH (range 10–13) obtained from P_r. **c**, Semilogarithmic plot of the disulfide-bond reduction rate as a function of the stretching force. Error bars show the s.e.m. reduction rate obtained at each particular pulling force, estimated using the bootstrapping method (see Methods). The reduction rate shows an abrupt change in force sensitivity at ~500 pN. Fits of the Arrhenius term $r(F) = r(0)\exp(F\Delta x_r/kT)$ to the experimental data (green squares) up to 500 pN give $\Delta x_r = 0.50$ Å (dotted grey line). A much smaller distance ($\Delta x_r = 0.11$ Å), which spans from 500 pN to 2 nN (dotted red line), is obtained when the experimental data are fitted to the high-force regime.

concentrations of hydroxide anions. We verified this by plotting the rate of reduction measured at 500 pN against the hydroxide anion concentration calculated from the pH of the solution (Fig. 3b). The data show that the rate of reduction follows an approximately first-order law that can be described as $r(F) = k(F)[OH^-]$. Thus, we can normalize the reduction-rate curves obtained at different pH values (Fig. 3a) by dividing the measured rates $r(F)$ by the concentration of hydroxide anions to give the reduction rate constant $k(F)$. Plots of $k(F)$ versus force show that the experimental data collapse into a single master curve, which clearly shows that the two distinct force regimes coexist at 500 pN (Fig. 3c).

The results presented here unambiguously demonstrate that the reduction of disulfide bonds by hydroxide anions exhibits an abrupt change in reactivity at a force of ~500 pN. However, is this a general mechanism or a particular feature of nucleophilic attack by hydroxide anions? To answer this we measured the force dependency of the rate of reduction with tris(2-carboxyethyl)phosphine (TCEP) as the nucleophile[19] over a wider force range up to 700 pN (crosses in Fig. 3c). Our experiments rely on the non-specific attachment of the protein between the surface and the cantilever tip. However, the probability of detachment from any of the ends is exponentially dependent on the stretching force. In the experiments with TCEP at neutral pH, it proved impossible to obtain data at forces higher than 700 pN because the polyproteins picked up by the AFM cantilever tip readily detached. The use of hydroxide anions in the measuring solution greatly enhanced the attachment of the polyprotein to the cantilever tip and the gold substrate, and thereby enabled exploration of the reaction mechanisms under a much-expanded range of pulling forces up to 2,000 pN, as demonstrated up to 1,400 pN in Fig. 3c. Despite these difficulties, the TCEP data to 700 pN also show an abrupt change in the slope at a force of ~500 pN, which demonstrates that the double-regime profile is not particular to hydroxide anions. We also examined whether the specific location of the disulfide bond within the structure of the I27 protein had a role in the switch in reactivity at 500 pN. We repeated the experiments reported in Fig. 1 with two other polyprotein constructs, $(I27_{E24C-K55C})_8$ and $(I27_{P28C-K54C})_8$, in which the cysteine mutations were engineered in different positions of the I27 sequence.

As before (Fig. 1), the reduction of a single, exposed disulfide bond is identified by a step increase in length that corresponds to the length of the amino acids trapped behind the disulfide bond. Disulfide-bond reductions cause step increases in length of ~10.4 nm for the $(I27_{E24C-K55C})_8$ construct and of ~8.8 nm for the $(I27_{P28C-K54C})_8$ construct (Supplementary Fig. S1).

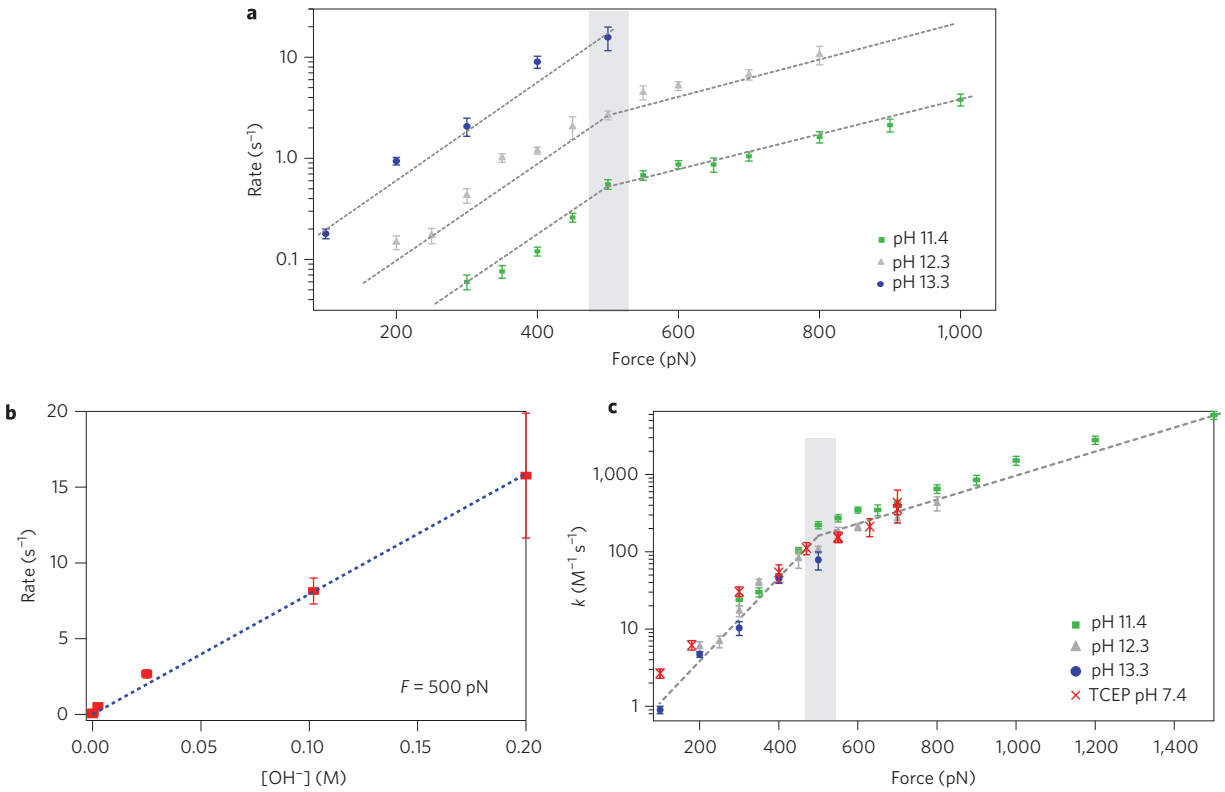

Figure 3 | The reactivity switch observed at a ~500 pN is a general mechanism in force-activated S_N2 reactions. a, Force dependency of the disulfide-bond reduction rate measured at three different values of pH (11.4, green squares; 12.3, grey triangles; 13.3, blue circles). Error bars show the s.e.m. reduction rate obtained at each particular pulling force, estimated using the bootstrapping method (see Methods). **b**, The rate of disulfide-bond reduction measured at 500 pN is linearly dependent on the hydroxide anion concentration [OH^-]. Thus, the reduction rate can be described by the equation $r(F) = k(F)[OH^-]$, where $k(F)$ is the rate constant of the reaction. **c**, Semilogarithmic plot of the rate constant of reduction $k(F)$ obtained by dividing the rates of reduction shown in Fig. 3a by the hydroxide anion concentration. The data collapse to a single master curve that clearly shows two different sensitivities to the applied force. The transition between the two regimes occurs in all cases at stretching forces ~500 pN (grey bar). The force dependency of the rate of reduction of disulfide bonds with the reducing agent TCEP (0.05–7.0 mM at pH = 7.4, red crosses) also shows an abrupt change in reactivity at ~500 pN, which suggests that the reactivity switch is independent of the nucleophile.

Figure 4a,b shows the force dependency of the rate of reduction for both constructs (Supplementary Fig. S2). Remarkably, the two-regime profile with a transition point around 500 pN was also found in the force dependency of the S_N2 reaction for disulfide bonds placed in different regions of the I27 protein. Fits of an Arrhenius term to the experimental data obtained from the $(I27_{E24C-K55C})_8$ construct gave $\Delta x_r = 0.46$ Å and $\Delta x_r = 0.07$ Å for the low- and high-force regimes, respectively (Fig. 4a). Fits to the experimental data obtained from the $(I27_{P28C-K54C})_8$ construct gave $\Delta x_r = 0.43$ Å and $\Delta x_r = 0.11$ Å for the low- and high-force regimes, respectively (Fig. 4b). These experiments were carried out at a pH value that kept the rate of reduction to within the limits of our spectrometer (see above). Interestingly, dividing the reduction rate by the concentration of hydroxide anions for each case resulted in reduction-rate constants $k(F)$ for all three polyprotein constructs that did not overlap (Fig. 4c). This demonstrates that the chemical environment around each particular disulfide bond has an important effect on the measured rate of reduction. However, in all cases, the abrupt mode switch is observed at ~500 pN (Fig. 4c, grey bar).

Discussion

Our single-molecule force-clamp assay directly measures fine details of the transition state of protein-based chemical reactions. For example, we measured Δx_r with sub-ångström resolution, which corresponds to the elongation of the S–S bond at the transition-state structure. Our results show that at a critical force of ~500 pN, the value of Δx_r decreases abruptly, which marks a drastic reduction in the sensitivity of the S_N2 reaction to the applied force. The vibrational frequency of a disulfide bond stretching mode is ~522 cm^{-1}, which predicts a bond-spring constant of ~255 N m^{-1} (ref. 22). Thus, a force of 500 pN would stretch this bond by only 0.02 Å and, furthermore, this elongation would be continuous with the applied force. Instead, we found an abrupt change in the elongation of the disulfide bond at the transition state, from $\Delta x_r \sim 0.50$ Å to $\Delta x_r \sim 0.10$ Å. We suggest two energy scenarios that are consistent with these results.

The first considers that the force-accelerated S_N2 chemical reduction of the disulfide bond is described by an energy profile composed of two consecutive energy barriers, an inner barrier close to the reactants along the reaction coordinate, and an outer barrier closer to the reaction products (Fig. 5a). In this scenario, the inner barrier has a Δx_{inner} of 0.1 Å and the outer barrier has a higher activation-energy barrier with $\Delta x_{outer} = 0.5$ Å. The outer barrier dominates the reaction in the low-force regime; however, given that the outer barrier is more sensitive to force, its activation energy (E_a) is more rapidly reduced until it is level with that of the inner barrier, at ~500 pN. Thus, at forces stronger than 500 pN the inner barrier, far less sensitive to the stretching force, becomes the rate-limiting step of the reaction (Fig. 5a). In this scenario, at ~500 pN both activation-energy barriers have similar size. From the extrapolation of the Arrhenius fit to the force dependency of the disulfide reduction rate (Fig. 2c), we can calculate the reduction rate in the absence of force, $r(0)$, for both force regimes, before and

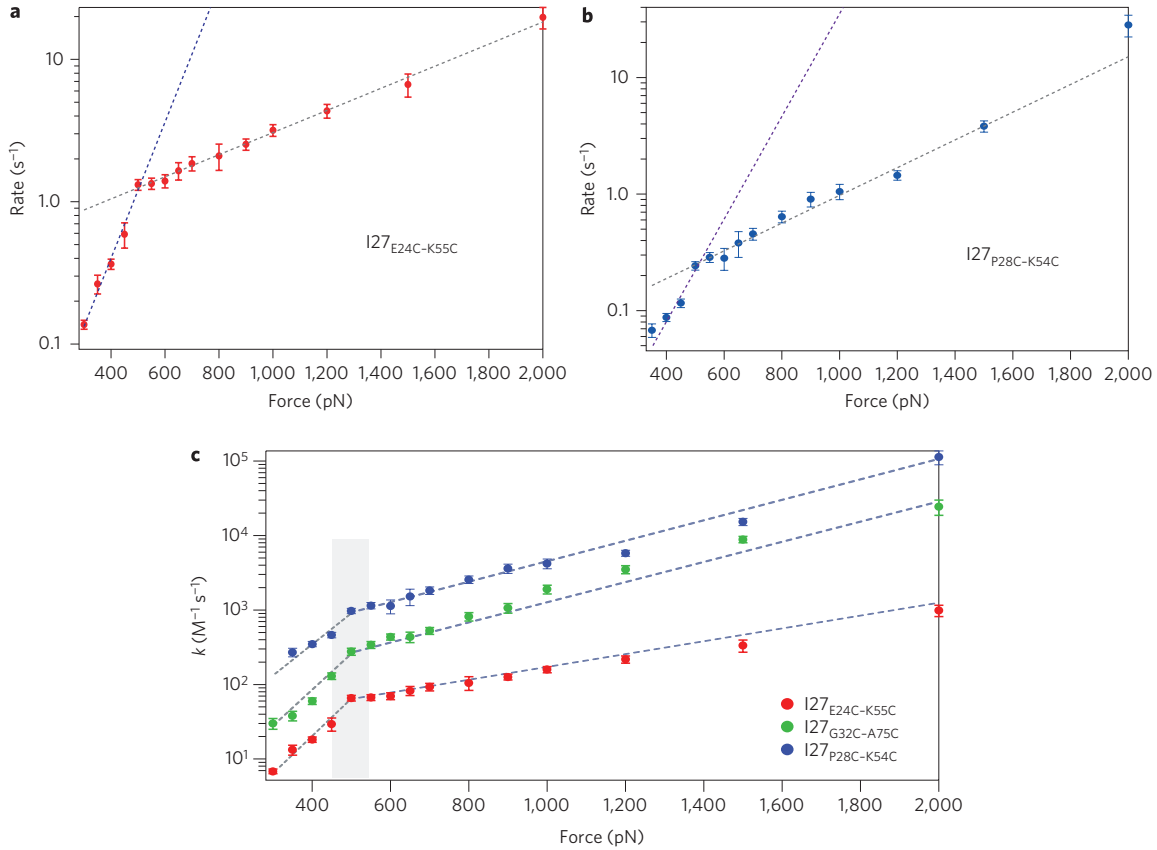

Figure 4 | The reactivity switch is independent of the location of the disulfide bond in the protein structure. a, Semilogarithmic plot of the reduction rate as a function of the pulling force for the $(I27_{E24C\text{-}K55C})_8$ construct (at pH 12.3). The Arrhenius fit to the experimental data in the low-force regime (dotted blue line) gives $\Delta x_r = 0.46$ Å, whereas the fit to the high-force regime (dotted grey line) gives $\Delta x_r = 0.07$ Å. **b**, Semilogarithmic plot of the reduction rate as a function of the pulling force for the $(I27_{P28C\text{-}K54C})_8$ construct (at pH 10.4). The Arrhenius fit to the experimental data in the low-force regime (dotted blue line) gives $\Delta x_r = 0.43$ Å, whereas the fit to the high-force regime (dotted grey line) gives $\Delta x_r = 0.11$ Å. **c**, Normalization of the data shown in Figs 2c, 4a and 4b by the hydroxide anion concentration results in an effective rate constant that is dependent on the location of the disulfide bond within the structure of the I27 protein. However, in all cases the reactivity switch is observed at ~500 pN (grey bar).

after the 500 pN transition. Given that $r(0) = A\exp(-E_a/k_BT)$, where k_B is the Boltzmann constant, we estimate the energy barriers that govern the process to be $E_{a,outer} = 86.1$ kJ mol^{-1} and $E_{a,inner} = 73.5$ kJ mol^{-1} ($\Delta E_a = 12.6$ kJ mol^{-1}), assuming that the same pre-exponential factor $A = 10^{12}$ M^{-1} s^{-1} applies in the two distinct force regimes. A molecular interpretation of this model implies that a nucleophile first collides with the disulfide bond to form a weak reactant complex that elongates the disulfide bond by ~0.1 Å. The formation of this complex requires desolvation of the reactants, which might be the origin of the first energy barrier (inner barrier in Fig. 5a). After forming the reactant complex, the reaction proceeds through its main energy barrier (outer barrier in Fig. 5a), which causes a further bond elongation of ~0.4 Å at the transition state of the reaction. This reaction scheme (Fig. 5a) is in qualitative agreement with the theoretical predictions applied to the particular case of an ion–molecule reaction in the condensed phase with asynchronous desolvation and ion–molecule complexation[23–25]. However, this model is inconsistent with the accepted view that a bimolecular nucleophilic displacement (S_N2) in solution occurs in a single, concerted step[26,27].

An alternative and more plausible explanation of our experimental results is that a mechanical force above 500 pN causes an abrupt conformational change in the substrate disulfide bond, which modifies its ground state. In this scenario there is a single activation-energy barrier for the S_N2 reaction, at which the shift in the ground state of the disulfide bond moves the reaction-energy barrier to a position closer to the transition-state structure (Fig. 5b). From this new bond geometry, acquisition of the transition state causes a much shorter bond elongation of ~0.1 Å, which accounts for the smaller force dependency observed in our experiments. A molecular interpretation of this view requires an understanding at the quantum chemistry level of the effects of a pulling force on a disulfide bond, which is unavailable at present. However, it is interesting that quantum calculations show that the CS–SC dihedral angle, χ, for open-chain disulfides is ~85° (refs 28, 29) and that changing χ from 85° to near 0° (*cis* conformation) or 180° (*trans* conformation) causes the disulfide bond S–S to lengthen by about 0.07 Å (refs 30–32). We speculate that when the force applied to the substrate disulfide bond reaches 500 pN, an abrupt conformational change drives the disulfide bond to a *trans* conformation, which elongates the C_α–C_α distance of the cysteine residues, and so reduces the overall energy of the molecule (Fig. 5c).

As discussed above, a disulfide bond in the *trans* conformation is longer than that in the *cis* conformation. It is possible that this lengthening is larger for a protein disulfide bond, and thus brings the ground state of the reaction closer to the transition state. It is likely that the force-induced *trans* geometry (Fig. 5c) results in a change of the degree of the disulfide bond exposure to the solution, which affects the new nucleophile-substrate orientation required for the 'backside' S_N2 reaction to proceed[33,34]. Remarkably, the calculated energy difference between both conformers ranges from ~7 to ~29 kJ mol^{-1} (refs 31,32,35), similar to the energy difference between the two barriers obtained from our experimental results,

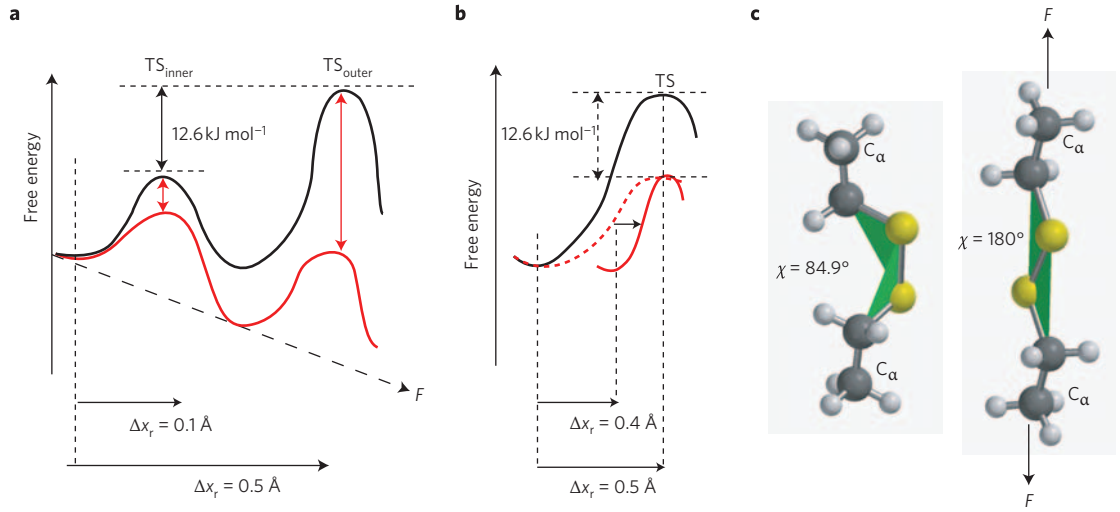

Figure 5 | Schematics of the two energy scenarios compatible with the experimental results. a, Energy profile of the S_N2 reaction for the two consecutive energy barriers. The outer energy barrier (TS_{outer}), with $\Delta x_r \sim 0.5$ Å, dominates the reaction in the low-force regime, and the inner energy barrier (TS_{inner}), much less sensitive to the pulling force ($\Delta x_r \sim 0.1$ Å), becomes rate-limiting above 500 pN. **b**, Energy profile of an S_N2 reaction limited by a single barrier. According to this scenario, at a force of ~500 pN the S–S bond undergoes a conformational change that shifts the ground state by 0.4 Å closer to the transition state (arrow). From this new geometry, the S–S bond elongates only by ~0.1 Å to reach the transition-state structure. **c**, Hypothetical model for of a conformational change induced by a mechanical stretching force that alters elongates the C_α–C_α distance of the cysteine residues and the dihedral angle χ (green planes) of a disulfide bond from the equilibrium conformation (yellow spheres, $\chi = 84.9°$) to the *trans* conformation ($\chi = 180°$).

$\Delta E_a = 12.6$ kJ mol^{-1}. Abrupt force-driven conformational changes in a single molecule are common, such as chair–boat conformational changes in single polysaccharide molecules that take place at a well-defined force[16,36]. For example, amylose molecules undergo force-driven chair–boat transitions at ~275 pN, whereas dextran molecules undergo these transitions at ~850 pN (refs 16,36,37). Thus, it is entirely plausible that a force of 500 pN triggers an abrupt change in the dihedral angle of the substrate disulfide bond.

Although both scenarios discussed here provide plausible explanations of our experimental results, other reaction mechanisms are worth considering. For example, it is plausible that, in addition to the S–S bond cleavage, C–S bond rupture occurs. Scission of the C–S bond is compatible with a bimolecular elimination mechanism induced by hydroxide anions[38]. In this scenario, the C–S bond breaks at low forces, and with increasing bond angles and dihedral angles, the S–S bond becomes more fragile or is more easily attacked by hydroxide anions. However, the observation that the reactivity switch is present at the same stretching force when TCEP is used as a nucleophile argues against this possibility. In addition, more complex mechanisms that involve both hydroxide anions and other molecules may also explain our data. For example, both ends of the breaking bond could react simultaneously under the effect of a pulling force[7,39,40], so hydroxide anions may react with one of the sulfur atoms, whereas the other sulfur atom binds to H_2O. This trimolecular reaction would help trigger the reaction at low forces. However, as it requires a very ordered transition state, it would not have a major role at high forces.

Single-molecule force-clamp spectroscopy is a novel experimental tool with which to study the sub-ångström changes in the transition-state structure of chemical reactions in the solution phase. Our experimental results provide the first demonstration that the application of a threshold mechanical force to the substrate of a bimolecular chemical reaction causes an abrupt change in reactivity. Although the existence of such a mechanochemical switch is clearly demonstrated by our experimental results, its molecular origins are still unknown. To establish the molecular mechanisms that underlie chemical reactions under force requires the development of quantum mechanical simulations modified to accept a mechanical stretching force as the driving perturbation[7,39–41]. Their development would positively impact our understanding on the mechanisms by which mechanical forces modulate chemical reactions, a mechanism that is widespread in nature.

Methods

Protein engineering. We used a cysteine-free I27 protein in which native Cys 47 and Cys 63, which do not form a disulfide bond, were mutated to alanines. Such constructs were the platform on which we engineered the I27 mutants used in this study. Using the QuickChange site-directed mutagenesis kit (Stratagene), we introduced additional mutations to form disulfide bonds at specific positions within the I27 protein sequence: Gly[32] to Cys, Ala[75] to Cys ($I27_{G32C–A75C}$); Pro[28] to Cys, Lys[54] to Cys ($I27_{P28C–K54C}$); Glu[24] to Cys, Lys[55] to Cys ($I27_{E24C–K55C}$). We constructed an eight-domain N–C linked polyprotein for each I27 mutant. Such polyproteins were engineered by consecutive subcloning of the respective monomers using the BamH I, Kpn I and Bgl II restriction sites. The eight-domain polyproteins were cloned into the pQE80L (Qiagen) expression vector and transformed into the BLR DE3 *Escherichia coli* expression strain. Each polyprotein construct was finally purified by histidine metal-affinity chromatography with Talon resin (Clontech) and by gel filtration using Superdex 200 HR column (GE BioSciences).

Force spectroscopy. Force-clamp AFM experiments were conducted at room temperature using a home-made set-up under force-clamp conditions described elsewhere[42]. The sample was prepared by depositing 1–10 μl of protein in PBS solution (at a concentration of 1–10 μg ml^{-1} for polyproteins) onto a freshly evaporated gold coverslide. Each cantilever (Si_3N_4 Veeco MLCT-AUHW) was individually calibrated using the equipartition theorem, which gave a typical spring constant of ~15 pN nm^{-1}. Single proteins were picked up from the surface by pushing the cantilever onto the surface with a contact force of 500–1,000 pN to promote the non-specific adhesion of the proteins on the cantilever surface. The piezoelectric actuator was then retracted to produce a set deflection (force), which was kept constant throughout the experiment using an external, active feedback mechanism while the extension was recorded. The force feedback was based on a proportional, integral and differential amplifier, the output of which was fed to the piezoelectric positioner. The feedback response is limited to ~3–5 ms. The high-resolution piezoelectric actuator gave our measurements of protein length a peak-to-peak resolution of ~0.5 nm. Data from the force traces were filtered using a pole Bessel filter at 1 kHz. Experiments with TCEP were conducted in a sodium phosphate buffer solution, specifically 50 mM sodium phosphate (Na_2HPO_4 and NaH_2PO_4), 150 mM NaCl, pH 7.4. Experiments at different pH values were conducted using buffer solutions of *N*-cyclohexyl-3-aminopropanesulfonic acid for pH 10–11.5 and phosphate buffer solution for pH 12–13.5. The final pH value in each solution was adjusted by adding the required amounts of NaOH or HCl solutions. Solutions were filtered through a 0.2-μm membrane prior to each experiment.

Data analysis. All data were recorded and analysed using custom software written in Igor Pro 5.0 (Wavemetrics). The fingerprint of a single polyprotein in our experiments was considered to be at least four well-resolved steps of the corresponding height in each construct during the first force pulse. No traces that included unfolding events during the second force pulse were included in the analysis. To obtain the reduction rate at each particular pulling force, we summed and normalized numerous ($n = 30$–100) reduction recordings for each particular pulling force. To obtain the reduction rate at each particular pulling force, we fitted the resulting averaged traces with single exponentials. To estimate the error on our experimentally obtained rate constants, we used the non-parametric bootstrap method[43]. At a given value of force, n staircases were randomly drawn with replacement from our original data set. These were summed and fitted to obtain a rate constant. This procedure was repeated 500 times for each data set, which resulted in a distribution that provided the s.e.m. reduction rate. The s.e.m. of $r(F)$ was used as the weighting factor when the $r(F)$ data were fitted to extract the values of Δx_r in the Arrhenius equation.

Received 12 January 2009; accepted 2 April 2009; published online 10 May 2009

References

1. Beyer, M. K. & Clausen-Schaumann, H. Mechanochemistry: The mechanical activation of covalent bonds. *Chem. Rev.* **105,** 2921–2948 (2005).
2. Hickenboth, C. R. *et al.* Biasing reaction pathways with mechanical force. *Nature* **446,** 423–427 (2007).
3. Beyer, M. K. Coupling of mechanical and chemical energy: proton affinity as a function of external force. *Angew. Chem. Int. Ed.* **42,** 4913–4915 (2003).
4. Grandbois, M., Beyer, M., Rief, M., Clausen-Schaumann, H. & Gaub, H. E. How strong is a covalent bond? *Science* **283,** 1727–1730 (1999).
5. Garnier, L., Gauthier-Manuel, B., van der Vegte, E. W., Snijders, J. & Hadziioannou, G. Covalent bond force profile and cleavage in a single polymer chain. *J. Chem. Phys.* **113,** 2497–2503 (2000).
6. Schmidt, S. W., Beyer, M. K. & Clausen-Schaumann, H. Dynamic strength of the silicon–carbon bond observed over three decades of force-loading rates. *J. Am. Chem. Soc.* **130,** 3664–3668 (2008).
7. Aktah, D. & Frank, I. Breaking bonds by mechanical stress: when do electrons decide for the other side? *J. Am. Chem. Soc.* **124,** 3402–3406 (2002).
8. Beyer, M. K. The mechanical strength of a covalent bond calculated by density functional theory. *J. Chem. Phys.* **112,** 7307–7312 (2000).
9. Liphardt, J., Onoa, B., Smith, S. B., Tinoco, I. & Bustamante, C. Reversible unfolding of single RNA molecules by mechanical force. *Science* **292,** 733–737 (2001).
10. Gore, J. *et al.* DNA overwinds when stretched. *Nature* **442,** 836–839 (2006).
11. Woodside, M. T. *et al.* Direct measurement of the full, sequence-dependent folding landscape of a nucleic acid. *Science* **314,** 1001–1004 (2006).
12. Neuman, K. C. & Nagy, A. Single-molecule force spectroscopy: optical tweezers, magnetic tweezers and atomic force microscopy. *Nature Methods* **5,** 491–505 (2008).
13. Rief, M., Gautel, M., Oesterhelt, F., Fernandez, J. M. & Gaub, H. E. Reversible unfolding of individual titin immunoglobulin domains by AFM. *Science* **276,** 1109–1112 (1997).
14. Kellermayer, M. S. Z., Smith, S. B., Granzier, H. L. & Bustamante, C. Folding–unfolding transitions in single titin molecules characterized with laser tweezers. *Science* **276,** 1112–1116 (1997).
15. Cecconi, C., Shank, E. A., Bustamante, C. & Marqusee, S. Direct observation of the three-state folding of a single protein molecule. *Science* **309,** 2057–2060 (2005).
16. Marszalek, P. E., Oberhauser, A. F., Pang, Y. P. & Fernandez, J. M. Polysaccharide elasticity governed by chair–boat transitions of the glucopyranose ring. *Nature* **396,** 661–664 (1998).
17. Wiita, A. P., Ainavarapu, S. R., Huang, H. H. & Fernandez, J. M. Force-dependent chemical kinetics of disulfide bond reduction observed with single-molecule techniques. *Proc. Natl Acad. Sci. USA* **103,** 7222–7227 (2006).
18. Ainavarapu, R. K. *et al.* Contour length and refolding rate of a small protein controlled by engineered disulfide bonds. *Biophys. J.* **92,** 225–233 (2007).
19. Ainavarapu, S. R. K., Wiita, A. P., Dougan, L., Uggerud, E. & Fernandez, J. M. Single-molecule force spectroscopy measurements of bond elongation during a bimolecular reaction. *J. Am. Chem. Soc.* **130,** 6479–6487 (2008).
20. Carrion-Vazquez, M. *et al.* Mechanical and chemical unfolding of a single protein: a comparison. *Proc. Natl Acad. Sci. USA* **96,** 3694–3699 (1999).
21. Garcia-Manyes, S., Brujic, J., Badilla, C. L. & Fernandez, J. M. Force-clamp spectroscopy of single-protein monomers reveals the individual unfolding and folding pathways of I27 and ubiquitin. *Biophys. J.* **93,** 2436–2446 (2007).
22. Lien-Vien, D., Colthup, N. B., Fateley, W. G. & Grasselli, J. G. *The Handbook of Infrared and Raman Characteristic Frequencies of Organic Molecules* 231–232 (Academic Press, 1991).
23. Bickelhaupt, F. M., Baerends, E. J. & Nibbering, N. M. M. The effect of microsolvation on E2 and S_N2 reactions: theoretical study of the model system $F^- + C_2H_5F + n$HF. *Chem. Eur. J.* **2,** 196–207 (1996).
24. Chandrasekhar, J., Smith, S. F. & Jorgensen, W. L. Theoretical examination of the S_N2 reaction involving chloride ion and methyl chloride in the gas phase and aqueous solution. *J. Am. Chem. Soc.* **107,** 154–163 (1985).
25. Chandrasekhar, J. & Jorgensen, W. L. Energy profile for a nonconcerted S_N2 reaction in solution. *J. Am. Chem. Soc.* **107,** 2974–2975 (1985).
26. Bohme, D. K. & Mackay, G. I. Bridging the gap between the gas phase and solution – transition in the kinetics of nucleophilic displacement reactions. *J. Am. Chem. Soc.* **103,** 978–979 (1981).
27. Brauman, J. I. Chemistry – Not so simple. *Science* **319,** 168–168 (2008).
28. Boyd, D. B. Sequence and shape of molecular-orbitals of disulfide HSSH. *J. Phys. Chem.* **78,** 1554–1563 (1974).
29. Boyd, D. B. Mapping electron density in molecules. 14. Nonbonded contacts between lone pairs on divalent sulfurs. *J. Phys. Chem.* **82,** 1407–1416 (1978).
30. Vanwart, H. E. & Scheraga, H. A. Stable conformations of aliphatic disulfides – influence of 1,4 interactions involving sulfur atoms. *Proc. Natl Acad. Sci. USA* **74,** 13–17 (1977).
31. Jiao, D., Barfield, M., Combariza, J. E. & Hruby, V. J. *Ab initio* molecular-orbital studies of the rotational barriers and the S-33 and C-13 chemical shieldings for dimethyl disulfide. *J. Am. Chem. Soc.* **114,** 3639–3643 (1992).
32. Vanwart, H. E., Shipman, L. L. & Scheraga, H. A. Variation of disulfide bond stretching frequencies with disulfide dihedral angle in dimethyl disulfide. *J. Phys. Chem.* **78,** 1848–1853 (1974).
33. Vollhardt, K. P. C. *Organic Chemistry* (Freeman, 2003).
34. Uggerud, E. Nucleophilicity – periodic trends and connection to basicity. *Chem. Eur. J.* **12,** 1127–1136 (2006).
35. Boyd, D. B. Electron redistribution in disulfide bonds under torsion. *Theor. Chim. Acta* **30,** 137–150 (1973).
36. Marszalek, P. E., Li, H., Oberhauser, A. F. & Fernandez, J. M. Chair–boat transitions in single polysaccharide molecules observed with force-ramp AFM. *Proc. Natl Acad. Sci. USA* **99,** 4278–4283 (2002).
37. Marszalek, P. E., Li, H. B. & Fernandez, J. M. Fingerprinting polysaccharides with single-molecule atomic force microscopy. *Nature Biotechnol.* **19,** 258–262 (2001).
38. Florence, T. M. Degradation of protein disulfide bonds in dilute alkali. *Biochem. J.* **189,** 507–520 (1980).
39. Lupton, E. M., Achenbach, F., Weis, J., Brauchle, C. & Frank, I. Molecular origins of adhesive failure: siloxane elastomers pulled from a silica surface. *Phys. Rev. B* **76,** 125420 (2007).
40. Lupton, E. M., Achenbach, F., Weis, J., Brauchle, C. & Frank, I. Origins of material failure in siloxane elastomers from first principles. *ChemPhysChem* **10,** 119–123 (2009).
41. Kruger, D., Fuchs, H., Rousseau, R., Marx, D. & Parrinello, M. Pulling monatomic gold wires with single molecules: an *ab initio* simulation. *Phys. Rev. Lett.* **89,** 186402 (2002).
42. Schlierf, M., Li, H. & Fernandez, J. M. The unfolding kinetics of ubiquitin captured with single-molecule force-clamp techniques. *Proc. Natl Acad. Sci. USA* **101,** 7299–7304 (2004).
43. Efron, B. *The Jacknife, the Bootstrap and Other Resampling Plans* (SIAM, 1982).

Acknowledgements

We thank L. Dougan, J. Alegre, P. Kosuri and other members of the Fernández laboratory for critical reading of the manuscript. S.G.-M. thanks the Generalitat de Catalunya for a postdoctoral fellowship through the NANO and Beatriu de Pinós programs, and also the Fundación Caja Madrid for financial support. This work was supported by NIH Grants (to J.M.F.).

Author contributions

S.G.M. and J.M.F. conceived and designed the experiments; S.G.M., J.L., R.S. and T.K. performed the experiments; S.G.M., J.L., R.S. and T.K analysed the data; S.G.M. contributed materials and analysis tools; S.G.M and J.M.F. wrote the paper.

Additional information

Supplementary information accompanies this paper at www.nature.com/naturechemistry. Reprints and permission information is available online at http://npg.nature.com/reprintsandpermissions/. Correspondence and requests for materials should be addressed to S.G.M. and J.M.F.